

where  $\delta_0$  is the level spacing for a particle of size  $a_0$ . In both the low- and high-temperature regions the particle-size distribution modifies only the coefficient of the leading temperature-dependent term and not the form of the power-law dependence.

\*Research sponsored by the U. S. Air Force Office of Scientific Research, Office of Aerospace Research, under Grant No. AFOSR-71-2007.

†National Science Foundation Senior Foreign Scientist. On leave from the Institut für Theoretische Physik der Universität zu Köln, Köln, Germany.

‡National Aeronautics and Space Administration Trainee.

<sup>1</sup>R. Kubo, J. Phys. Soc. Jap. **17**, 975 (1962).

<sup>2</sup>L. P. Gor'kov and G. M. Eliashberg, Zh. Eksp. Teor. Fiz. **48**, 1407 (1965) [Sov. Phys. JETP **21**, 940 (1965)].

<sup>3</sup>Some small-particle effects have already been observed. See for example C. Taupin, J. Phys. Chem. Solids **28**, 41 (1967); S. Kobayashi *et al.*, Phys. Lett. **33A**, 429 (1970).

<sup>4</sup>E. P. Wigner, ORNL Report No. ORNL-2309, 1957

(unpublished), p. 54.

<sup>5</sup>F. J. Dyson, J. Math. Phys. **3**, 140 (1962).

<sup>6</sup>C. E. Porter, *Statistical Theories of Spectra: Fluctuations* (Academic, New York, 1965).

<sup>7</sup>M. L. Mehta, *Random Matrices and Statistical Theory of Energy Levels* (Academic, New York, 1967).

<sup>8</sup>A simple estimate gives  $\eta \approx (\hbar v_F/a)(\Delta g)^2$ , where  $\Delta g$  is the electron  $g$  shift: A. Kawabata, J. Phys. Soc. Jap. **29**, 902 (1970).

<sup>9</sup>S. Tomonaga, Progr. Theor. Phys. **5**, 544 (1950).

<sup>10</sup>H. Fröhlich, Physica (Utrecht) **4**, 406 (1937).

<sup>11</sup>In these calculations we approximate the  $n$ -level spacing distribution for Dyson's three ensembles by Wishart distributions (see Refs. 6 and 7). The Wigner function is just the single-spacing Wishart distribution corresponding to the orthogonal case.

<sup>12</sup>We estimate that the first-order approximation is good to within 10% for the Dyson ensembles and 20% for the Poisson case over the entire temperature range. Asymptotically at both low and high temperatures the error becomes completely negligible for our purposes and is caused by the small deviation of the finite-level-spacing Wishart distributions from the exact ones. See for example Fig. 1.3 of Ref. 7.

## Interpretation of Low-Energy Electron-Diffraction Spectra for a Free-Electron Metal in Terms of Multiple Scattering Involving Strong Inelastic Damping\*

S. Y. Tong and T. N. Rhodin

*Department of Applied Physics, Cornell University, Ithaca, New York 14850*

(Received 18 January 1971)

The multiple-scattering approach with strong inelastic damping has been used to formulate low-energy electron-diffraction intensity curves without the use of adjustable parameters. The results have been applied to the interpretation of spectra for the clean (001) face of aluminum with good agreement. Inclusion of energy-dependent higher order phase shifts obtained from a realistic potential, of energy-dependent strong inelastic damping, and of temperature effects contributes significantly to the agreement of the calculation with experiment.

The elastic and inelastic scattering of low-energy electrons provides a powerful approach to the study of the atomic structure and electron properties of crystal surfaces. Encouraging progress has been made recently in the development of theoretical approaches to the problem.<sup>1-9</sup> Recognition of the importance of strong inelastic damping contributed significantly to this development.<sup>1-6</sup> Duke and Tucker<sup>1</sup> were the first to provide effectively for this contribution in a phenomenological way in terms of the multiple-scattering approach. Using an  $s$ -wave model, they expressed the scattering and damping factors in terms of adjustable parameters, and they were able to interpret important qualitative features

of the intensity profiles observed in low-energy electron diffraction (LEED).<sup>1</sup>

In this Letter, we wish to report on the first complete calculation of LEED spectra for a free-electron metal in terms of the multiple-scattering approach involving strong inelastic damping with no adjustable parameters. The significance of this work is that within the constraints inherent to the approach it produces spectral curves in meaningful agreement with specific details of experimental results obtained by Jona<sup>10</sup> for a relatively simple metal, aluminum, when we compare to the detailed conditions of his measurement. Specifically, resonance effects associated with strong intraplanar scattering were

found to make a major contribution to the multiple-scattering features. It is indicated that LEED spectra for which the above considerations are applicable present the distinct possibility of providing meaningful information on the atomic geometry of the surface layer. This is probably one of the most important single objectives of current studies in the application of the LEED approach to the surface physics of crystals.

The inelastic-scattering approach of Duke and Tucker<sup>1,2</sup> is used with the following three major modifications. First, in addition to using the *s*-wave phase shift, characteristic of their calculations, the higher order phase shifts are included. The contribution of the higher order phase shifts to the scattering potential is of great importance in a realistic calculation. Known calculations on some metals (e.g., tungsten<sup>8,9</sup> and iron<sup>8</sup>) show a strong *d*-type ( $l=2$ ) resonance dominating the ion-core scatterings at energies 20 eV and above. Second, emphasis is placed on using energy-dependent phase shifts derived from the Pendry-Capart scattering potential<sup>4,5</sup> constructed in the muffin-tin approximation for the LEED energy range. Third, the strong inelastic damping due to single-particle and bulk-plasmon excitations is explicitly provided for by use of the self-energies<sup>11</sup> calculated for an interacting homogeneous electron gas. The loss mechanism due to surface-plasmon excitations<sup>12</sup> is not included in this work. The inclusion of such an absorption term due to surface-plasmon losses into our present scattering model calls for introducing a position- and angle-dependent parameter. We chose to exclude the use of such a parameter in our present calculation. Finally, essential temperature corrections to the results calculated at absolute zero are put in by use of the vertex renormalization approach of Duke and Laramore.<sup>13</sup> In summary, the objective of this Letter is to show that within the context of the multiple-scattering model it is necessary to provide explicitly for the higher order phase shifts and the strong inelastic damping to obtain good agreement between the calculated spectra and details of the measured spectra. When this is done, meaningful interpretation of the contribution of multiple scattering to the primary and secondary spectral structures can be achieved.

In an interacting electron gas, a quasiparticle satisfies the dispersion relation

$$\hbar^2 \vec{k}^2 / 2m = E - \Sigma^*(\vec{k}, \hbar^2 \vec{k}^2 / 2m, Z(\vec{k})), \quad (1)$$

where<sup>11</sup>

$$\Sigma^*(\vec{k}, \hbar^2 \vec{k}^2 / 2m, Z(\vec{k})) = Z(\vec{k}) \Sigma(\vec{k}, E = \hbar^2 \vec{k}^2 / 2m) + \epsilon_0 [1 - Z(\vec{k})]. \quad (2)$$

$\Sigma(\vec{k}, E = \hbar^2 \vec{k}^2 / 2m)$  is the electron self-energy calculated in an effective (random-phase approximation) interaction between the electrons, and  $Z(\vec{k}) = [1 - \partial \Sigma(\vec{k}, \hbar^2 \vec{k}^2 / 2m) / \partial E]^{-1}$  is a complex renormalization factor.  $\epsilon_0 = \Sigma(k_F, \hbar^2 k_F^2 / 2m)$  is a shift in energy related to the chemical potential level.<sup>11</sup> The self-consistent solution of Eq. (1), solved by always putting the real part of the solution  $\vec{k}$  on the right-hand side of (1), leads to the complex term  $k_1 + ik_2$ . The imaginary part  $\Sigma_2^*$  of  $\Sigma^*$  represents the total damping effects due to bulk-plasmon and single-particle excitations. It increases rapidly at the bulk-plasmon threshold, reaches quickly a value of 5 eV, and stays almost constant from then on. In the region where  $\Sigma_2^*$  stays almost constant (50-200 eV),<sup>14</sup> the electron mean free path<sup>15</sup>  $\lambda = (\hbar^2 / 2m)(2k_1 / |\Sigma_2^*|)$  varies approximately as  $E^{1/2}$ .

The effects of ion-core scattering in the multiple-scattering method are expressed in terms of energy-dependent phase shifts.<sup>16</sup> In the *s*-wave model,<sup>1,2</sup> the consideration that the ion cores are simply *s*-wave scatterers is perhaps one of the more limiting assumptions of their model. Besides the fact that real potentials are not isotropic scatterers, an important defect is that the scattering amplitudes calculated in the *s*-wave approximation are much too small. Previous calculations using *s*-wave phase shift<sup>17</sup> found it necessary to multiply the *s*-wave scattering amplitude by a constant in order to account for the strong ion-core effect. The importance of the higher order phase shifts is augmented by the fact that each *l*th-order scattering matrix is weighed by the multiplicity factor  $2l + 1$ . Because of the lack of a good scattering potential expressed in terms of phase shifts applicable in the LEED energy region, previous phase-shift calculations were either based on neutral atom models<sup>8</sup> or restricted to near the Fermi level.<sup>9</sup> The first scattering potential to our knowledge that is constructed for the LEED energy region and is explicitly expressed in terms of energy-dependent phase shifts was proposed by Pendry<sup>18</sup> and Capart.<sup>5</sup> In this work we have calculated the first six phase shifts for aluminum in the energy range 0-180 eV based on a program by Pendry.<sup>18</sup> At about 24 eV, the  $l=2$  (*d*-type) partial wave becomes highly dominant. A recent aug-

mented plane-wave calculation by Connolly<sup>19</sup> on aluminum reported a *d*-band resonance at the same energy. In Fig. 1, we show the first four phase shifts of aluminum as functions of incident electron energy. The  $l \geq 4$  phase shifts are not shown in the figure.

The elastic intensity of a given reflected beam for given incident energy and direction is given by<sup>16</sup>

$$I(\vec{k}, \vec{k}') = N(E)(2m/\hbar^2)(4\pi)^2 \left| \sum_{LL'} Y_L(\vec{k}) Y_{L'}^*(\vec{k}') \sum_{\nu} \exp[i(\vec{k} - \vec{k}') \cdot \vec{d}_{\nu}] [T_{\nu}]_{LL'} \right|^2 \delta_{\vec{k}_{\parallel}, \vec{k}'_{\parallel} + \vec{g}_{\parallel}}, \quad (3)$$

where  $N(E)$  is an energy-dependent normalization coefficient,<sup>20</sup>  $L(l, m)$  is the index of the partial-wave expansion, and  $d_{\nu}$  is the vertical distance of the  $\nu$ th layer from the surface plane. The matrices  $[T_{\nu}]_{LL'}$  satisfy a set of coupled equations<sup>16</sup> and are related to the planar-scattering matrices  $[\tau_{\nu}]_{LL'}$ , which for a single site is  $t_l(\kappa) = -(h^2/2m) [\exp(2i\delta_l) - 1]/2i\kappa$ , via structural propagators  $[G^{\nu\nu'}(\vec{k})]_{LL'}$  and  $[G^{\nu\nu}(\vec{k})]_{LL'}$ , respectively. We evaluate the elements of  $[T_{\nu}]_{LL'}$  by perturbation theory.<sup>2</sup> The use of this approach greatly simplifies the computation and increases its speed, and its accuracy is within the limits imposed by the interpretation of the experimental data. Our use of the perturbation method is adequate for the main purpose of this Letter which is to interpret the primary and secondary features of the LEED spectra with peak widths of order 10-18 eV. Interpretation of the fine structure of individual peaks, for example, requires further investigation of higher-order perturbation and will be considered elsewhere.<sup>20</sup> The temperature effects are put in by multiplying the ion-core scattering matrix  $t_l(\kappa)$  by the "Debye-Waller" factor defined in Ref. 13. As a first-order approximation, only the *s*-wave expansion of the "Debye-Waller" factor is used.

The LEED spectra for the (00) beam at normal

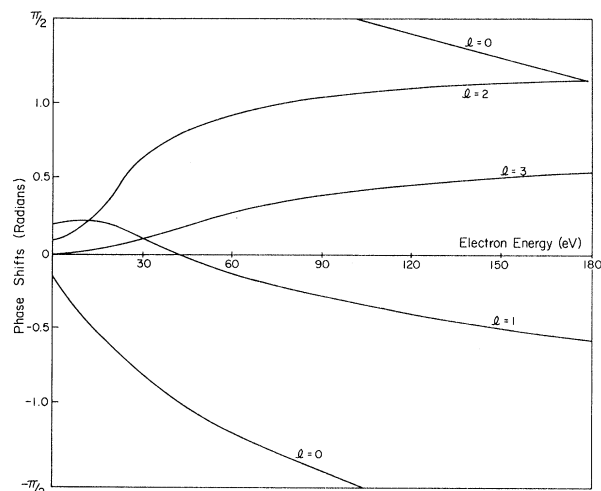


FIG. 1. The first four phase shifts of aluminum expressed modulo  $\pi$ , plotted in the energy range 0-180 eV.

incidence on (001) aluminum for two temperatures (4.2 and 293°K) are shown in Figs. 2(a) and 2(b). We notice large shifts in peak positions

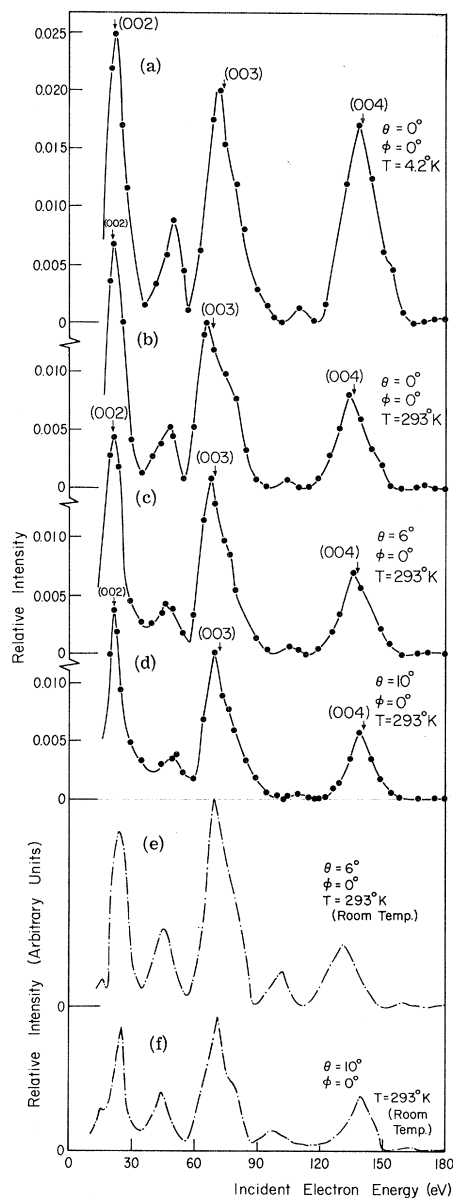


FIG. 2. (a)-(d) The calculated LEED spectra for Al (001). The curves are drawn by joining the calculated values (dots) with a smooth line. (e), (f) The experimental results of Jona, Ref. 10.

(due mostly to thermal expansion) and large decreases in peak intensities with increasing temperature. The decrease in peak intensities is larger at higher energies. Putting in the factor  $N(E) = 1/(A_0^2 \kappa^2)$ ,<sup>20</sup> where  $A_0$  is the area of the two-dimensional unit cell, the main peak heights agree roughly with the formula  $e^{-2W}|f|^2/E$ .<sup>21</sup>

The (00)-beam spectral curves for two other angles of incidence are shown in Figs. 2(c) and 2(d). The curves were calculated at 20°C and these were compared with the normalized data of Jona,<sup>10</sup> shown in Figs. 2(e) and 2(f), taken at room temperature. The calculated intensities are given in absolute reflectivities. The surface of the electron gas is placed at a distance  $a_z = a_0/2$  ( $a_0$  = lattice constant) from the centers of the surface-row atoms. Absorption of the incident beam passing through this layer of electron gas was taken into account. Approximately, this surface-layer absorption reduces the final reflectivity by a factor of  $\frac{1}{3}$ . The absolute reflectivities of most of the spectral peaks are of the order of 1.5% or less. The peak widths are in the range 10–18 eV. This is in marked contrast with results<sup>7</sup> based on a purely elastic calculation. Both the smallness (of order no larger than a few percent) of the absolute reflectivities and the very wide half-widths are direct consequences of the strong inelastic damping.

The effects of the intraplanar scattering in terms of  $[\tau_{LL'}]$  are illustrated in Fig. 3. In the case of *s*-wave scattering  $|\tau_{00}|^2$  has minima at the threshold energies of new low-index beams<sup>1,22</sup> [Fig. 3(b)].  $||G^{vv}(\vec{k})_{00}|$  has maxima at these energies {and in the case of purely elastic theory,  $||G^{vv}(\vec{k})_{00}| \rightarrow \infty$ .<sup>22</sup> In the case of higher-order phase shifts, the elements of the complex matrix  $[G^{vv}(\vec{k})]_{LL'}$  have different phase factors according to the values  $L, L'$ . When the sum of their inverses is taken in the factor  $|\sum_{LL'} \tau_{LL'} Y_L(\vec{k}) Y_{L'}^*(\vec{k}')|^2$ , the different phase factors tend to cancel the terms in the sum. The net effect is that most minima are smoothed out and broad regions of strong intraplanar resonances are produced as indicated in Fig. 3(a). A study of the LEED spectra in Fig. 2(b) and of the planar-scattering features in Fig. 3(a) shows that by mapping the simple kinematic Bragg peaks at their proper energies onto the intraplanar features in Fig. 3(a), one can account for most of the primary and secondary spectral structures. The planar-scattering structures are very sensitive to the atomic geometry of a single layer of atoms. The broad regions of strong intraplanar resonance due to

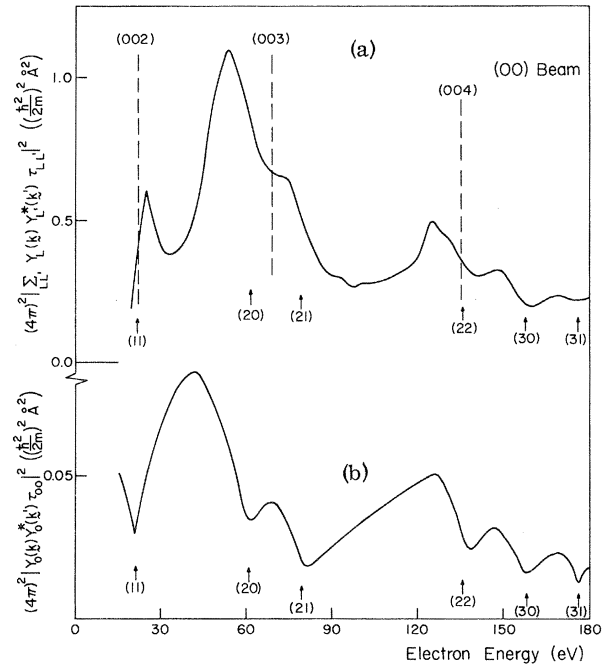


FIG. 3. The magnitudes of the intraplanar scattering matrices (a) for multiple phase shifts and (b) just the *s*-wave phase shifts. The vertical arrows indicate the emergence energies of the index beams shown in parenthesis. The dotted lines indicate the kinematic Bragg-peak energies.

higher-order phase shifts and the fact that these planar structures are mostly determined by the atomic geometry of a single layer suggest that this is a very useful way to predict surface atomic geometry from LEED intensity spectra.

In summary, it is shown, for a simple metal, that good agreement can be obtained in the multiple-scattering approach with proper inclusion of higher-order phase shifts and of inelastic damping. No adjustable parameters need to be included. This now provides an effective approach for structure analysis of surface layers and overlayers and of effects of temperature from LEED spectra for simple metals.

The authors are grateful to J. B. Pendry for the use of his program on phase-shift calculations and to F. Jona for his data on aluminum spectra prior to publication. Helpful discussions with B. I. Lundqvist, J. B. Pendry, J. W. Wilkins, and N. W. Ashcroft are gratefully acknowledged.

It has been brought to our attention, since this paper was submitted, that independent calculations of comparable LEED spectra by D. Jepsen, P. Marcus, and F. Jona, using a different approach, are in good agreement with these results.

\*Work supported by the U. S. Air Force Office of Scientific Research, Grant No. 68-1586, and by the Advanced Research Projects Administration through the Cornell Materials Science Center.

<sup>1</sup>C. B. Duke and C. W. Tucker, Jr., *Phys. Rev. Lett.* **23**, 1163 (1969); *Surface Sci.* **15**, 231 (1969). For discussion of structure analyses within the spirit of the *s*-wave model see C. W. Tucker, Jr., and C. B. Duke, *Surface Sci.* **23**, 411 (1970), and **24**, 31 (1971); C. B. Duke and G. E. Laramore, *Phys. Rev. B* **2**, 4765, 4783 (1970).

<sup>2</sup>C. B. Duke, J. R. Anderson, and C. W. Tucker, Jr., *Surface Sci.* **19**, 117 (1970).

<sup>3</sup>R. O. Jones and J. A. Strozier, Jr., *Phys. Rev. Lett.* **22**, 1186 (1969); J. A. Strozier, Jr., and R. O. Jones, *Phys. Rev. Lett.* **25**, 516 (1970).

<sup>4</sup>J. B. Pendry, *J. Phys. C: Proc. Phys. Soc., London* **2**, 1215, 2273, 2283 (1969).

<sup>5</sup>G. Capart, "Dynamical Calculations of LEED Intensities at Clear Copper (001) Surface (to be published).

<sup>6</sup>R. M. Stern and F. Balibar, *Phys. Rev. Lett.* **25**, 1338 (1970).

<sup>7</sup>V. Hoffstein and D. S. Boudreaux, *Phys. Rev. Lett.* **25**, 512 (1970).

<sup>8</sup>K. Kambe, *Surface Sci.* **20**, 213 (1970).

<sup>9</sup>P. J. Jennings and E. G. McRae, *Surface Sci.* **23**, 363 (1970).

<sup>10</sup>F. Jona, *IBM J. Res. Develop.* **14**, 444 (1970).

<sup>11</sup>B. I. Lundqvist, *Phys. Status Solidi* **32**, 273 (1969).

<sup>12</sup>J. I. Gersten, *Phys. Rev. B* **2**, 3457 (1970).

<sup>13</sup>Duke and Laramore, Ref. 1.

<sup>14</sup>All energy scales quoted are measured with respect to the vacuum level, unless otherwise specified.

<sup>15</sup>Our definition of  $\lambda (=k_2^{-1})$  is the same as that defined in Ref. 2 and is twice that defined in the first paper of Ref. 1.

<sup>16</sup>J. L. Beeby, *J. Phys. C: Proc. Phys. Soc., London* **1**, 82 (1968).

<sup>17</sup>B. W. Holland and R. W. Hannum, to be published.

<sup>18</sup>J. B. Pendry, private communication.

<sup>19</sup>J. W. D. Connolly, in *Proceedings of the Symposium on Atomic, Molecular, and Solid-State Theory and Quantum Biology*, edited by P. Löwdin (Interscience, New York, 1969), p. 807.

<sup>20</sup>S. Y. Tong and T. N. Rhodin, to be published.

<sup>21</sup>M. G. Lagally and M. B. Webb, *Phys. Rev. Lett.* **21**, 1388 (1968).

<sup>22</sup>E. G. McRae, *J. Chem. Phys.* **45**, 3258 (1966).

## Simple Theory of the Magnetic Properties of Rare-Earth Metals

L. M. Falicov and C. E. T. Goncalves da Silva\*

*Department of Physics, † University of California, Berkeley, California 94720*

(Received 18 January 1971)

A simple theory for the magnetism of the rare-earth metals is presented. It is based on assuming strongly correlated, well-defined *f*-electron states of an atomiclike character which are weakly hybridized with conduction-band states. This hybridization plays the role of an indirect exchange interaction. A model calculation is presented: It yields for various values of the two relevant parameters ferromagnetic, antiferromagnetic, and helical arrangements. These arrangements are strongly dependent on the features of the conduction-electron band structure (Fermi surface). Order of magnitude estimates give reasonable agreement for physical parameters as determined from unrelated experiments.

We report here a simple theoretical model which explains qualitatively the many possible magnetic arrangements of the rare-earth metals.<sup>1</sup> In this model the usual roles of hybridization between *f*-like and conduction-band wave functions and correlation effects between *f*-like electrons are reversed, i.e., the correlation effects are taken into account as the important, zeroth-order contribution to the energy and the *f*-state-conduction-band hybridization terms are included as a perturbation.

The same zeroth-order Hamiltonian has been used successfully<sup>2</sup> to explain the  $\alpha$ - $\gamma$  phase transition in cerium metal. It assumes that the *f* levels and the conduction band are not hybridized.

The conduction states are essentially noninteracting Bloch states derived from the 6*s* and 5*d* states of the atom. The localized *f* states are atomiclike (or ioniclike to be more precise) in character and are strongly correlated to one another, constituting on the whole a well-defined many-electron structure with well-defined total angular momentum *J*. The energetics of this structure is such that, for all phenomena involved here, only one electron can be either removed from an *f* shell and placed (really or virtually) in a conduction state or vice versa. If, for the sake of definiteness and simplicity, we assume that only occupations with zero or one *f* electron are permitted, or zero or one *f* hole as well, corre-